SUPPLEMENTAL INFORMATION

Supplementary Table 1- Subcutaneous tumor formation with M1, M2, M3 and M4 cell lines in Balb/c nude mice

Cell line	*Number of mice developing tumor/Number of mice used*	*Tumor incidence (%)*
MCF10A (M1)	0/12	0%
MCF10A-HRAS^{G12V} (M2)	10/12	83%
MCF10ACA1h (M3)	12/12	100%
MCF10CA1a.cl1 (M4)	12/12	100%

Supplementary Table 2- Primers used for the ChIP-PCR assay:

1. SLC5A8_ChIP 1: 5'-ACTCAGGGCAGCGGGTCGAT-3' (forward)
   5'-AGCCCTGCGCGCAAACTG-3' (reverse)
2. SLC5A8_ChIP 2: 5'-AACGTGCCAAGCATGTATGT-3' (forward)
   5'-TCAACAGTCCGGGTCCTT-3' (reverse)
3. SLC5A8_ChIP 3: 5'-ATTTGGCTGGAGCGTCTATT-3' (forward)
   5'-CATACATGCTTGGCACGTTT-3' (reverse)
4. SLC5A8_ChIP 4: 5'- ACATCAGACACCCGAAAG-3' (forward)
   5'-GGGCTACTGTAAGTTATGGC-3' (reverse)

Supplementary Table 3- Primers used for the RT-PCR assay:

1. Human SLC5A8: 5'-GGCGATTGGGTACCGAGATAA-3' (forward)
   5'-AGTCTACAGCAAGGCGAGCAT-3' (reverse)
2. Human DNMT1: 5'-GGCTCCGCAAATGCTACGA-3' (forward)
   5'-CGCCAGACG AGACCAATCATC-3' (reverse)
3. Human DNMT3a: 5'-GTGGAAGGAAATTTGCGTGTGG-3' (forward)
   5'-GCCTCATTCAGCTCTCGGAACAT-3' (reverse)
4. Human DNMT3b: 5'- CGCCTTC TCTCCGTCCTC-3' (forward)
   5'-TTCAACTGTTCTCGTCGTTTCC-3' (reverse)
5. Human GAPDH: 5'-TGGACCTGACCTGCCGTCTA-3' (forward)
   5'-AGGAGTGGGTGTCGCTGTTG-3' (reverse)
6. Mouse Slc5a8: 5'-TTATGGGCGGTCGCAGTA-3'(forward)
   5'-CAGAGGCCCACAAGGTTGACAT-3' (reverse)
7. Mouse Dnmt1: 5'-AGTGTGGCCAGCACCTAGAC-3'(forward)
   5'-CCTTGGCTTCGTCGTAACTC-3' (reverse)
8. Mouse Dnmt3a: 5'-GCTACATGTGCGGGCATAAG-3'(forward)
   5'-CATGCAGGAGGCGGTAGAAC-3' (reverse)
9. Mouse Dnmt3a: 5'-CGGAATGCGCTGGGTACAGT-3'(forward)
   5'-GAAGCGATCCCGGCAACTCT-3' (reverse)
10. Mouse HPRT1: 5'-GCGTCGTTAGCGATGATGAAC-3'(forward)
    5'-CCTCCCATCTCCTTCATGACATCT-3' (reverse)

Supplementary Table 4- Primers used for Genotype

1. MMTV-Hras-Tg: 5'-CCC AGG GCT TAA GTA AGT TTT TGG-3' (forward)

   5'-GGG CAT AAG CAC AGA TAA AAC ACT-3' (reverse)

2. MMTV-Hras-IC: 5'-CAA ATG TTG CTT GTC TGG TG-3' (forward)

   5'-GTC AGT CGA GTG CAC AGT TT-3' (reverse)

3. MMTV-Slc5a8-Tg: 5'-CACGCGTCCGTGGCT-3' (forward)

   5'-GAGCCTAAATACCTGTTGCCAA-3' (reverse)

Supplementary Figures:

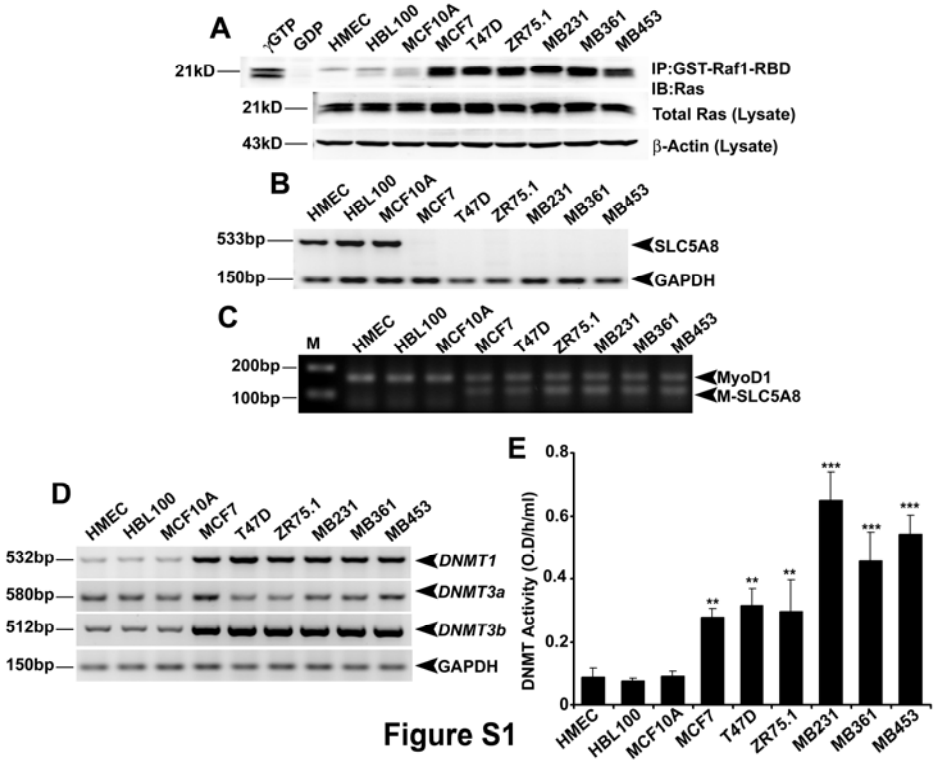

Figure S1

FIG S1 SLC5A8 expression is inversely correlated with oncogenic HRAS, DNMT gene expression and DNMT enzymatic activity. (A) RAS kinase assay demonstrates that RAS expression was activated in human breast cancer cells when compared to human non-transformed normal mammary epithelial cells. (B) RT-PCR analyses show that SLC5A8 expression was silenced in human breast cancer cells when compared to non-transformed normal mammary epithelial cells. (C) MS-PCR analysis reveals that SLC5A8 gene was methylated in all human breast cancer cells. (D) RT-PCR analysis demonstrates that DNMT1 and DNMT3b gene transcripts were induced in breast cancer cells when compared to non-transformed normal mammary epithelial cells. GAPDH was used as an internal control. (E) DNMT enzymatic assay shows that DNMT enzymatic activity was significantly high in human breast cancer cells when

compared to non-transformed normal mammary epithelial cells. Data are shown as a means ± SEM for three independent experiments.

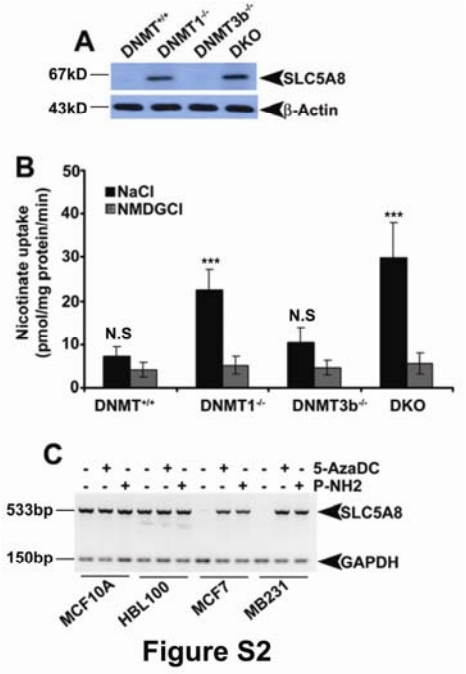

Figure S2

FIG S2 DNMT1-knockdown re-activates *SLC5A8* expression. (A) Western blot analysis confirms the induction of SLC5A8 protein in *DNMT1*$^{-/-}$ and DKO (*DNMT1*$^{-/-}$/*DNMT3b*$^{-/-}$)-knockdown cells. (B) Na^+-dependent uptake of ^{14}C-nicotinate shows an increase in SLC5A8 functional activity in *DNMT1*$^{-/-}$ and DKO (*DNMT1*$^{-/-}$/*DNMT3b*$^{-/-}$)-knockdown cells. Data are shown as a means ± SEM for three independent experiments. (C) RT-PCR analysis demonstrates the induction of SLC5A8 expression by inhibition of DNMTs, using either the pan-DNMT inhibitor 5-Aza-2-deoxycytidine (5-AzaDC) or DNMT1-specific inhibitor procainamide ($P\text{-}NH_2$) in human breast cancer cells.

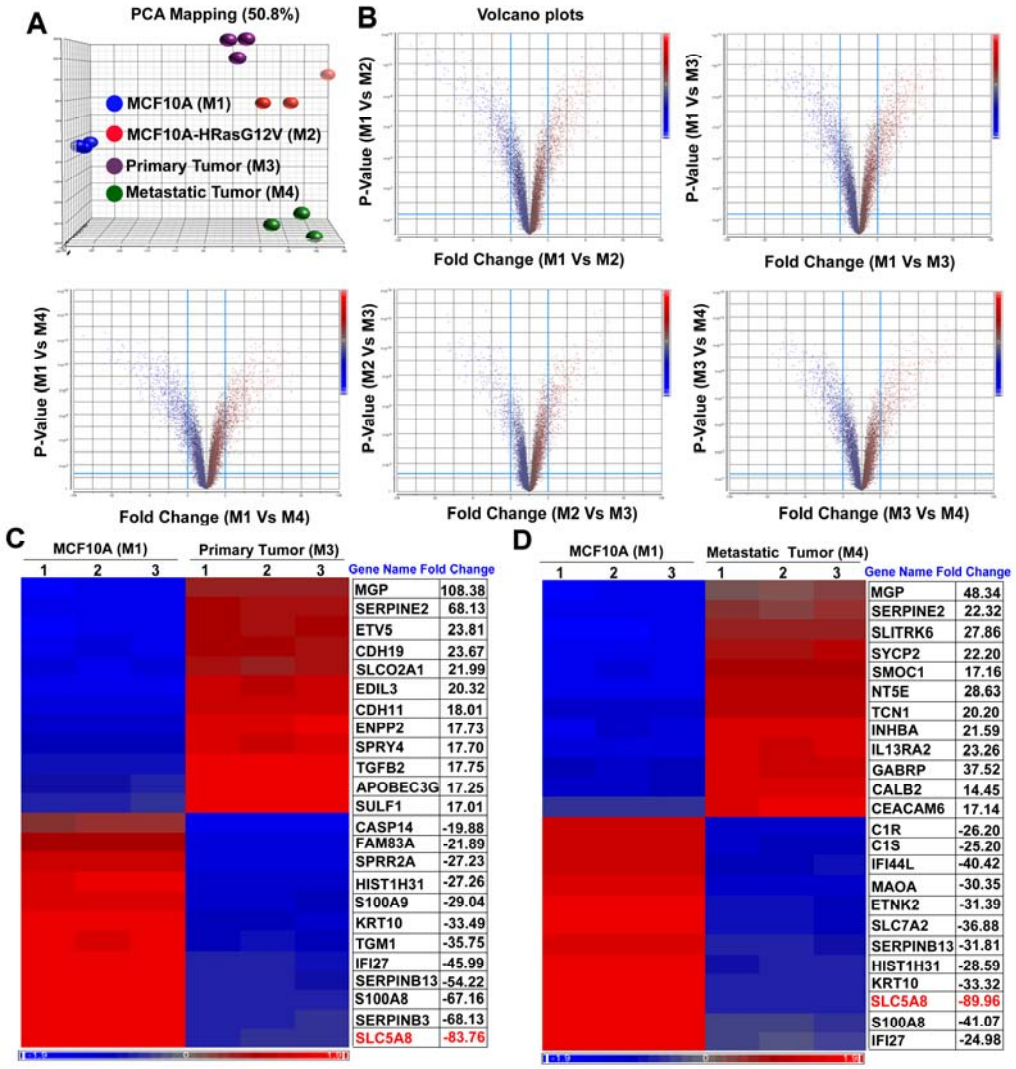

Figure S3

FIG S3 SLC5A8 inactivation is an early event in HRAS-induced cellular transformation and mammary tumor progression. **(A)** PCA mapping shows the relative gene expression in triplicate samples of M1, M2, M3 and M4. (B) Volcano plots show the differential gene expression between M1 vs. M2; M1 vs. M3; M1 vs. M4; M2 vs. M3 and M3 vs. M4. (C) Heat map demonstrates the 12 highly upregulated genes and 12 highly downregulated genes between M1 vs. M3 and M1 vs. M4.

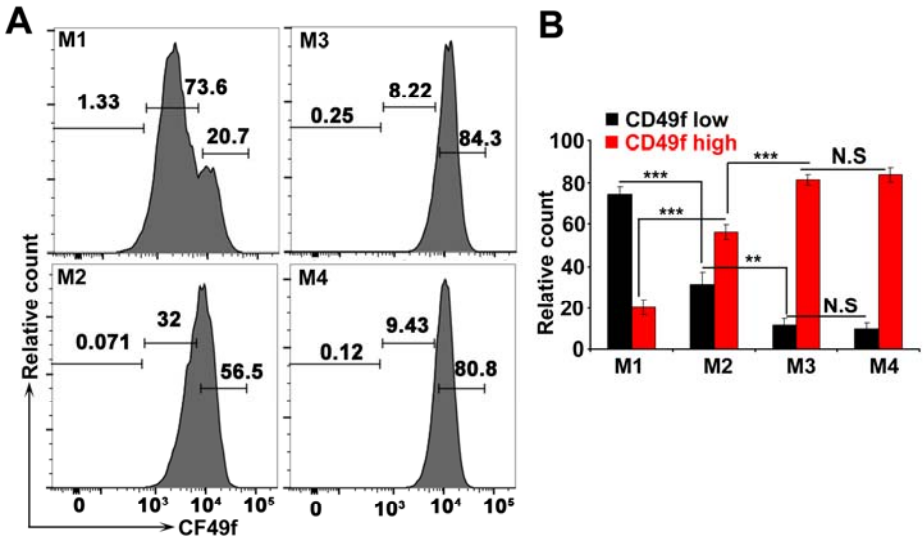

Figure S4

FIG S4 Increased CD49f expression in M2, M3 and M4 Cells. (A) Flow cytometry analysis showing increased CD49f population in M2, M3 and M4 when compared to M1 cells. (B) Quantitative representation of $CD49f^{low}$ and $CD49f^{high}$ populations in M1, M2, M3 and M4 cells. Data are shown as means ± SEM for three independent experiments. **p<0.01; ***p<0.001; N.S = Not significant by t-test.

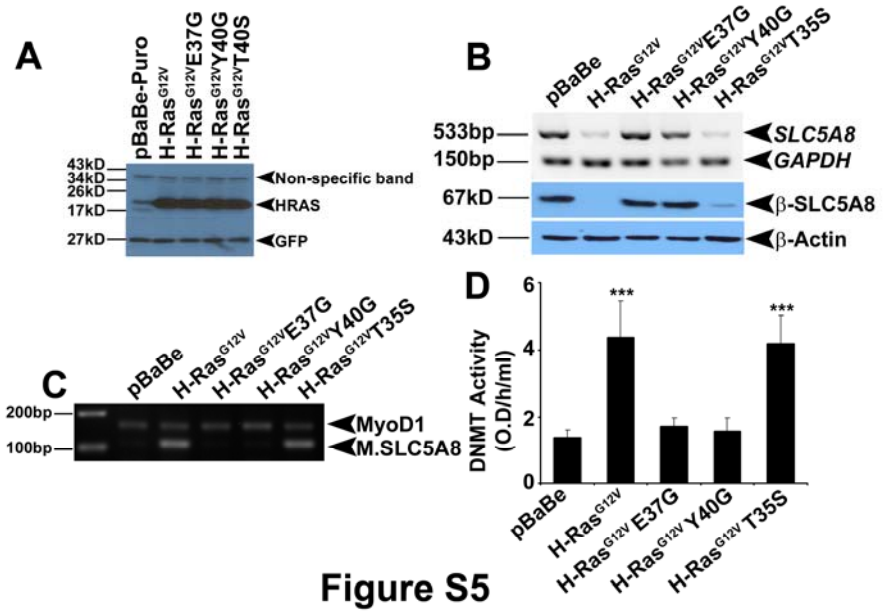

Figure S5

FIG S5 RAS/RAF/ERK signaling pathway is involved in SLC5A8 inactivation. (A) Western blot analysis for HRAS and GFP expression demonstrates the equal expression of all HRAS mutants in MCF10A cells. (B) RT-PCR and western blot analyses demonstrate *SLC5A8* gene transcript and protein expression was silenced by oncogenic HRAS ($HRAS^{G12V}$) and RAF/ERK activating mutant $HRAS^{G12V}$T35S in MCF10A cells. (C) MS-PCR demonstrates that *SLC5A8* methylation was induced by oncogenic $HRAS^{G12V}$ and $HRAS^{G12V}$T35S in MCF10A cells. (D) Induction of DNMT enzymatic activity by $HRAS^{G12V}$ and $HRAS^{G12V}$T35S in MCF10A cells. Data are shown as means ± SEM for three independent experiments. ***$p<0.001$ by t-test.

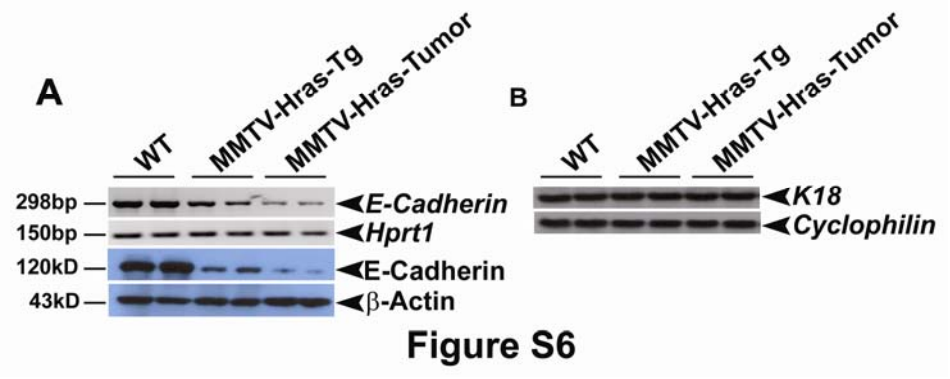

FIG S6 Comparable epithelial content in normal, MMTV-Hras premalignant and tumor tissues. (A) Western blot analysis for E-cadherin showing that expression of E-cadherin is down regulated in MMTV-Hras premalignant and tumor tissues when compared to normal mammary gland and suggesting that E-cadherin may not be an appropriate epithelial marker in our experiment. (B) Northern blot analysis for keratin 18 (K18) showing a comparable expression in normal and MMTV-Hras premalignant and tumor tissues. Cycliophilin was used as an internal control.

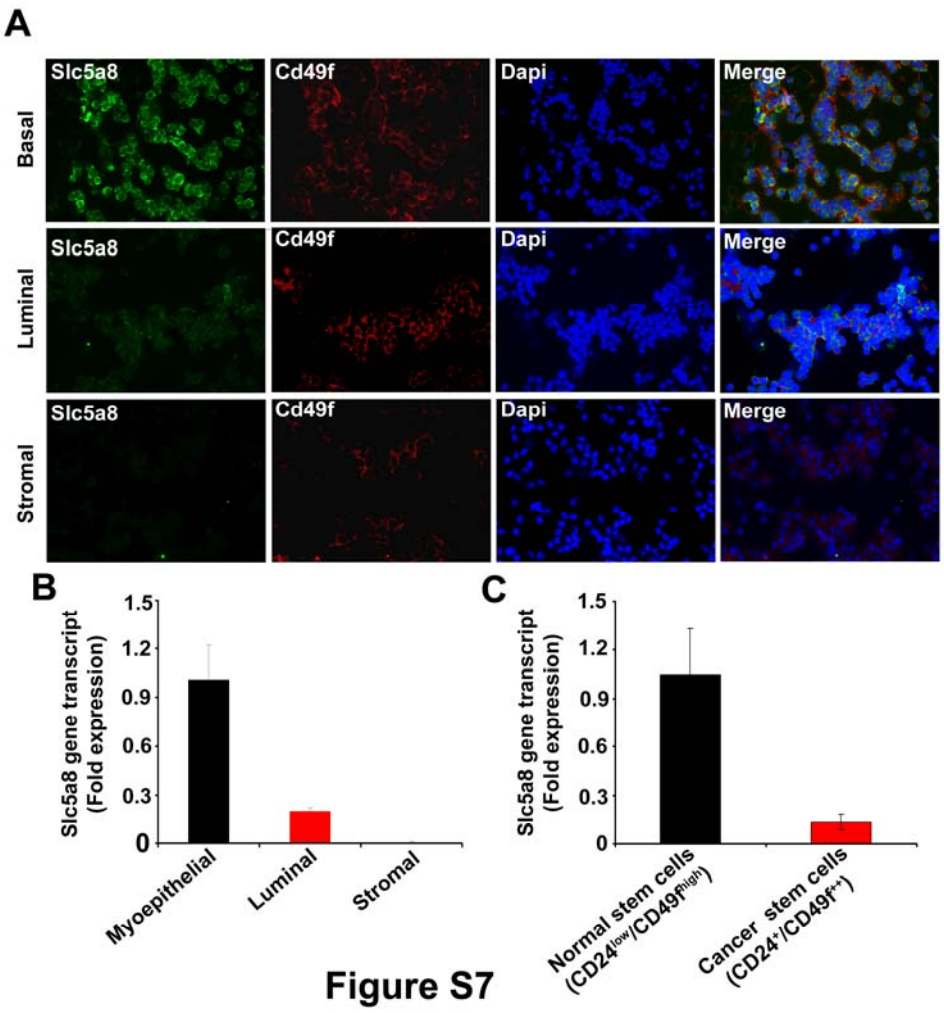

FIG S7 Slc5a8 is expressed in basal mammary epithelial cells. (A) Immunofluorescence analysis of Slc5a8 (green) in basal ($Lin^-CD49^{hi}CD24^{low}$), luminal ($Lin^-CD49f^{low}CD24^{hi}$) and stromal ($Lin^-CD49f^-CD24^-$) cell population, which isolated from normal mammary gland, showing that it is mainly expressed in basal, relative low expression in luminal and not expressed in stromal cell types. We also used CD49f (red) and Dapi (blue). (B). Real-time PCR analysis showing Slc5a8 is highly expressed in basal cell type than luminal and stromal cells. Data are shown as means ± SEM for three independent experiments. ***$p<0.001$ by t-test.

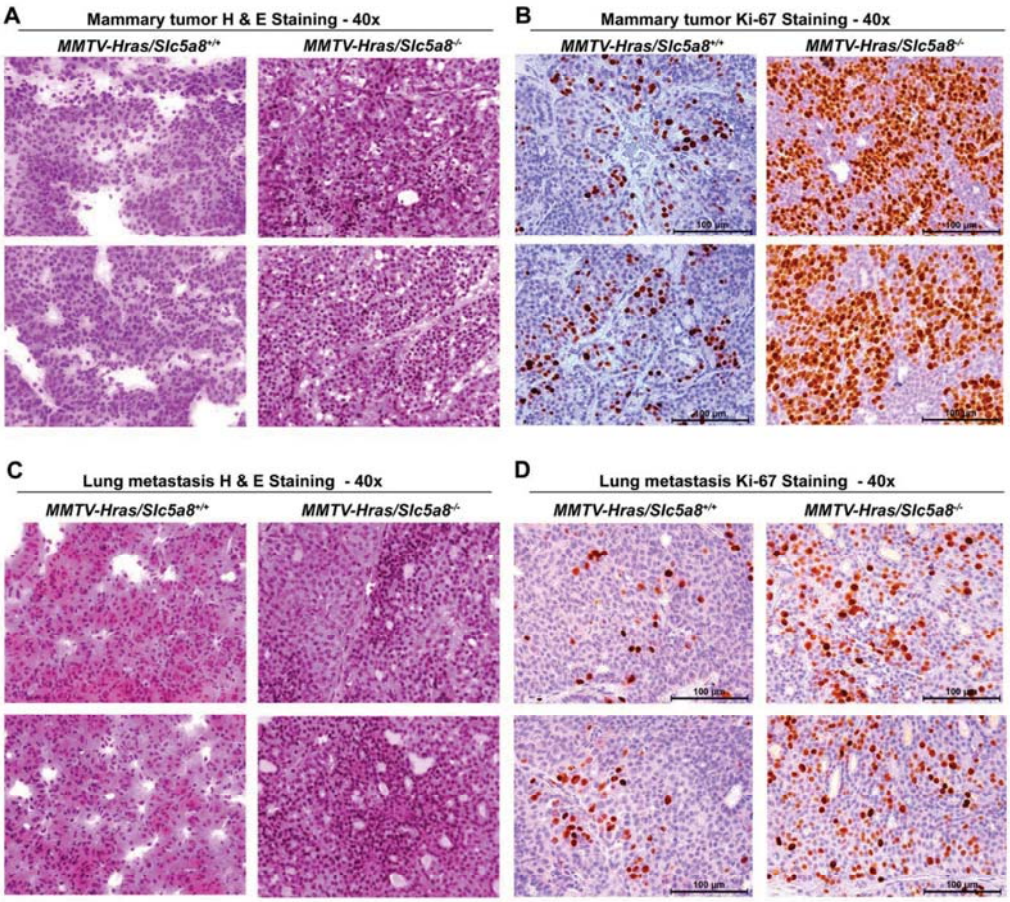

Figure S8

FIG S8 Deletion of *Slc5a8* in mice is associated with aggressive tumor phenotype. (A) Representative H & E images of mammary tumor tissues from *MMTV-Hras*/*Slc5a8*$^{+/+}$-Tg mice and *MMTV-Hras*/*Slc5a8*$^{-/-}$-Tg mice. Data show that highly invasive and infiltrating ductal carcinoma occurred in *MMTV-Hras*/*Slc5a8*$^{-/-}$-Tg mice whereas in *MMTV-Hras*/*Slc5a8*$^{+/+}$-Tg mice tumors were less proliferative and locally invasive ductal carcinoma in situ (DCIS). Ki-67 staining supports the highly invasive and aggressive tumor phenotype in *MMTV-Hras*/*Slc5a8*$^{-/-}$-Tg mice. (B) H & E sections of lung metastatic tissues from *MMTV-Hras*/*Slc5a8*$^{+/+}$-Tg mice and *MMTV-Hras*/*Slc5a8*$^{-/-}$-Tg mice demonstrate the highly invasive and infiltrating tumor phenotype in *MMTV-Hras*/*Slc5a8*$^{-/-}$-Tg mice. Ki-67 staining supports the highly invasive and aggressive tumor phenotype in *MMTV-Hras*/*Slc5a8*$^{-/-}$-Tg mice. Images from two mice are shown here.

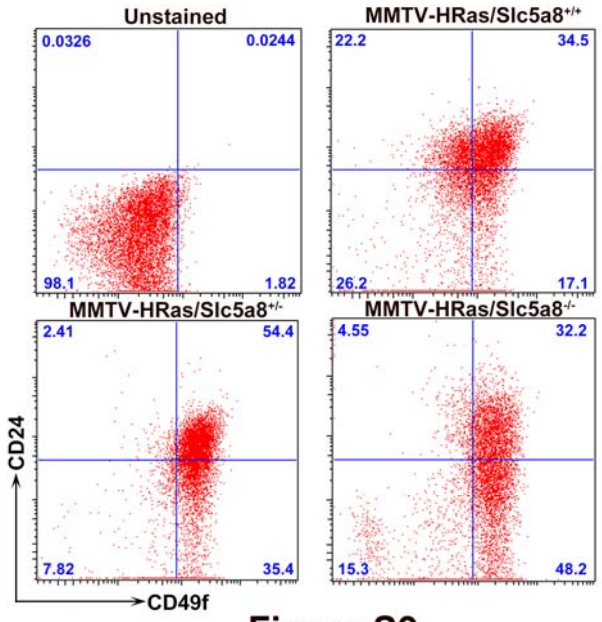

Figure S9

FIG S9 Deletion of *Slc5a8* is associated with increased tumor-initiating cancer stem cell formation in MMTV-Hras-Tg mice. FACS data demonstrate a dose-dependent increase in cancer-initiating stem cells ($Lin^{-}CD49f^{high}$ $CD24^{low}$) (lower right quadrant) upon deletion of *Slc5a8* (*Slc5a8*$^{+/+}$, *Slc5a8*$^{+/-}$ and *Slc5a8*$^{-/-}$) in MMTV-Hras-Tg mice.

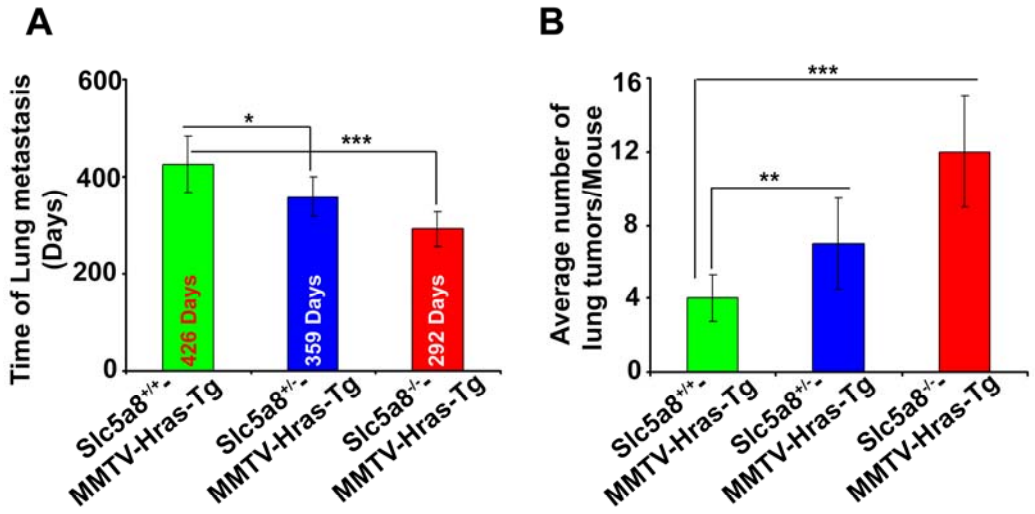

Figure 10

FIG S10 Deletion of *Slc5a8* is associated with early onset of lung metastasis with increased metastatic nodules. (A) Early onset of lung metastasis of mammary tumor in *Slc5a8*$^{-/-}$-*MMTV-Hras*/-Tg mice compared to *Slc5a8*$^{+/+}$-*MMTV-Hras*-Tg mice and *Slc5a8*$^{+/-}$-*MMTV-Hras*/-Tg mice. *p<0.05; ***p<0.001 by t-test. (B) Increased number of visible lung tumors (nodules) in *Slc5a8*$^{-/-}$-*MMTV-Hras*/-Tg mice when compared to *Slc5a8*$^{+/+}$-*MMTV-Hras*-Tg mice and *Slc5a8*$^{+/-}$-*MMTV-Hras*/-Tg mice. **p<0.01; ***p<0.001 by t-test.

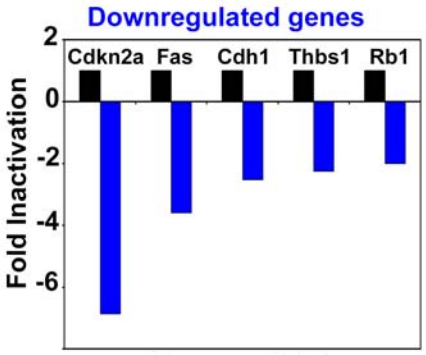

Figure S11

FIG S11 Deletion of *Slc5a8* is associated with downregulation of tumor suppressor genes in MMTV-Hras-Tg mouse tumor. Downregulation of indicated genes, which are involved in cell cycle regulation and tumor suppression, in *Slc5a8*$^{-/-}$*-MMTV-Hras-Tg* mouse tumors compared to tumors from *Slc5a8*$^{+/+}$*-MMTV-Hras-Tg* mice (number of mice in each group = 3).

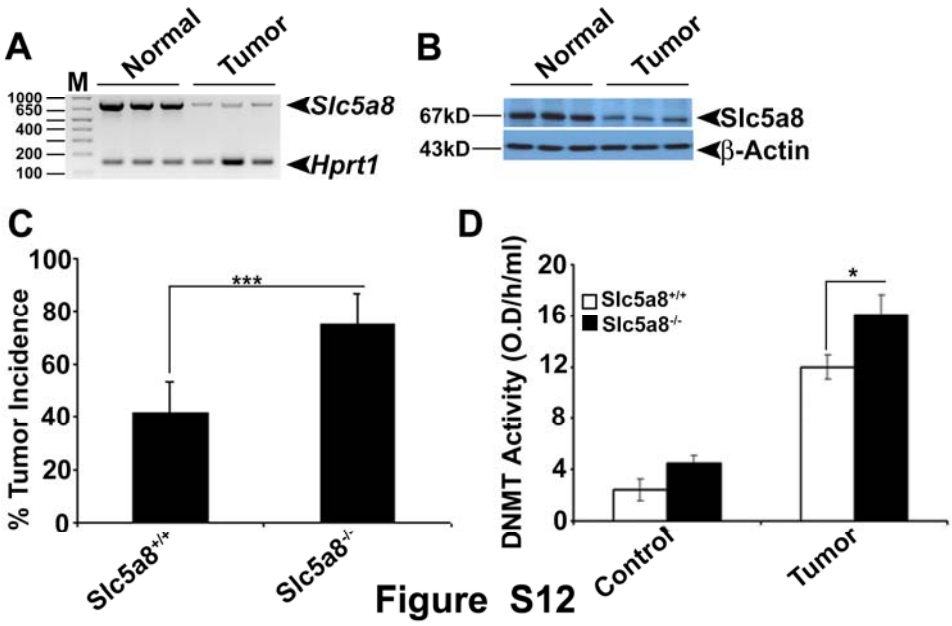

Figure S12

FIG S12 Deletion of *Slc5a8* sensitizes to carcinogen-induced mammary tumorigenesis in mice. (A) RT-PCR provides evidence for silencing of *Slc5a8* in mammary tumors induced by the carcinogen DMBA. Hprt1 was used as an internal control. (B) Western blot analysis provides evidence for decreased expression of SLC5A8 protein in mammary tumors induced by DMBA. (C) Tumor incidence in wild type mice and in *Slc5a8*$^{-/-}$ mice in response to DMBA exposure, providing evidence for increased occurrence of mammary tumors in *Slc5a8*$^{-/-}$ mice compared to wild type mice. Data are means ± SEM of three independent experiments. ***$p<0.001$ by t-test. (D) Comparison of DNMT enzymatic activity in normal mammary gland and in DMBA-induced mammary tumors between wild type mice and *Slc5a8*$^{-/-}$ mice. Data are means ± SEM of three independent experiments. *$p<0.01$; by t-test.

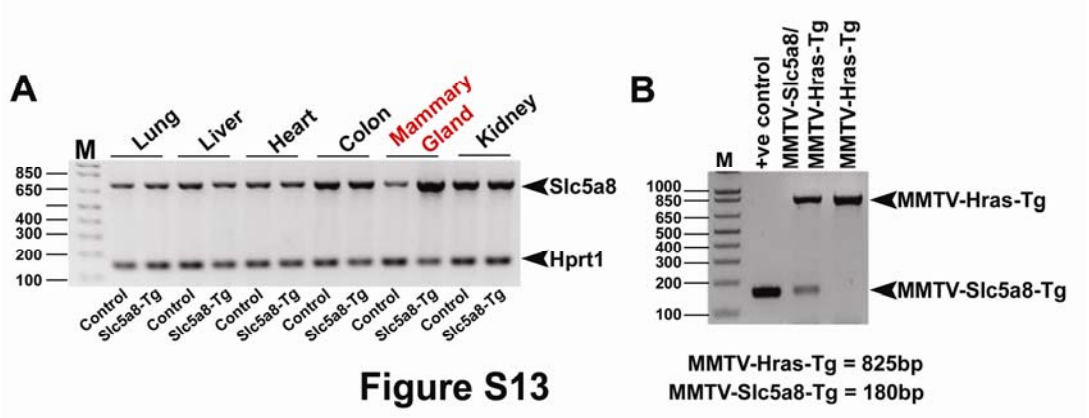

FIG S13 Selective overexpression of Slc5a8 in mammary gland *MMTV-Slc5a8*-Tg mice. (A) RT-PCR showing mammary gland-specific overexpression of *Slc5a8* gene transcript in *MMTV-Slc5a8*-Tg mice. (B) RT-PCR providing evidence for the expression of Hras and Slc5a8 in mammary glands from *MMTV-Hras*/*MMTV-Slc5a8* double-transgenic mice. As a positive control for Slc5a8, we used the plasmid construct that was employed for generation of the *MMTV-Slc5a8*-Tg mouse.

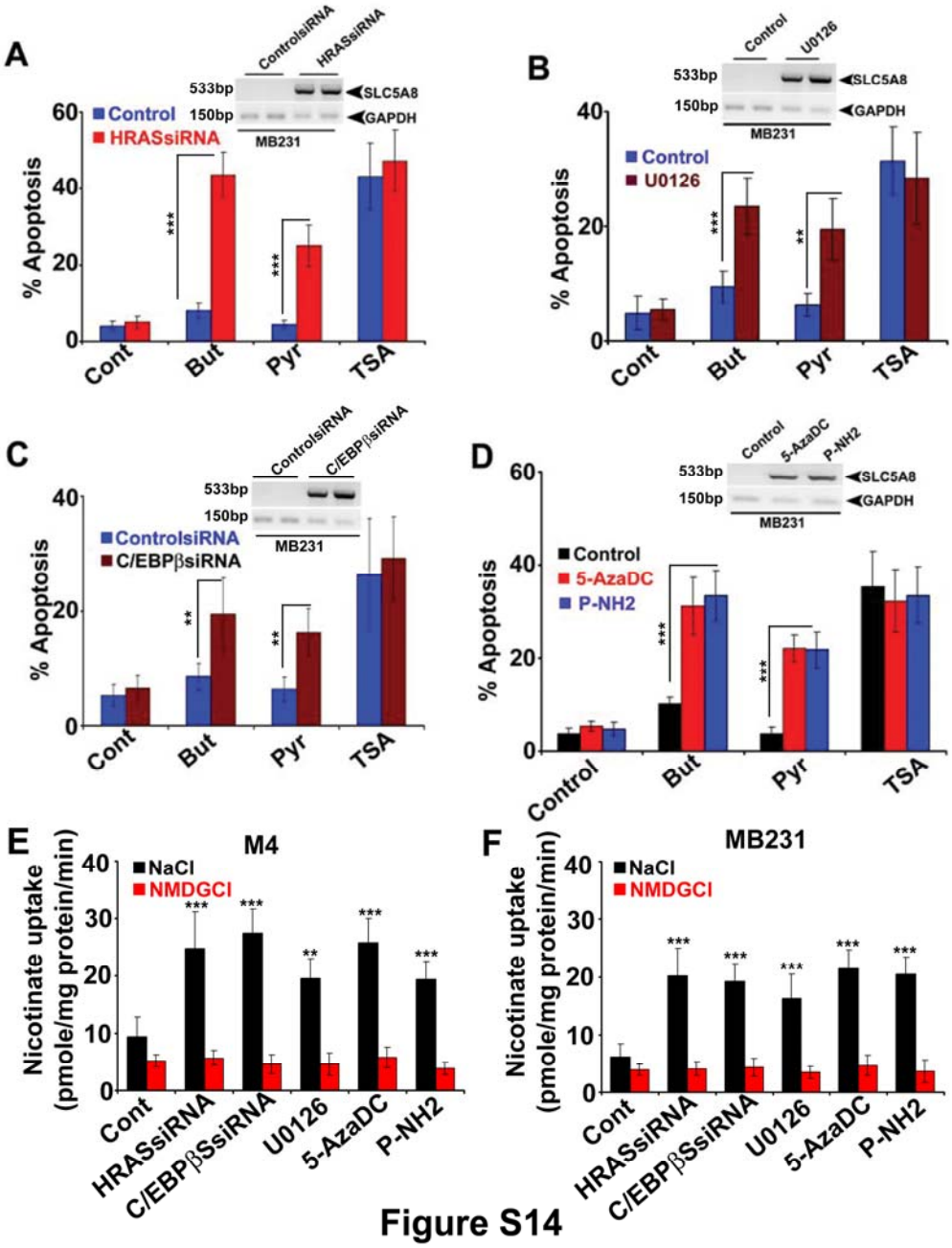

Figure S14

FIG S14 Inhibition of HRAS signaling and DNMTs re-activates SLC5A8 expression and function that induces apoptosis in the human breast cancer cell lines. (A) RT-PCR showing evidence for increased expression in SLC5A8 in MB231 cells in response to siRNA-induced downregulation of HRAS (Inset). FACS analysis demonstrating induction of apoptosis in MB231 cells, which were engineered to upregulate SLC5A8 expression by siRNA-induced

silencing of HRAS and then exposed to butyrate or pyruvate (SLC5A8 substrates as well as HDAC inhibitors). TSA was used as a positive control. (B) RT-PCR showing evidence for increased expression of SLC5A8 in MB231 cells in response to blockade of MRK/ERK pathway (Inset). FACS analysis demonstrating induction of apoptosis in MB231 cells, which were engineered to upregulate SLC5A8 expression by treatment with an inhibitor of MRK/ERK signaling (U0126) and then exposed to butyrate or pyruvate. (C) RT-PCR showing evidence for increased expression in SLC5A8 in MB231 cells in response to siRNA-induced downregulation of C/EBPβ (Inset). FACS analysis demonstrating induction of apoptosis in MB231 cells, which were engineered to upregulate SLC5A8 expression by siRNA-induced silencing of C/EBPβ and then exposed to butyrate or pyruvate. (D) RT-PCR showing re-activation of SLC5A8 expression in MB231 cells when treated with the DNMT inhibitors 5'-aza-2-deoxycytidine (5-AzaDC) or procainamide (P-NH_2) (Inset). FACS analysis demonstrating induction of apoptosis in MB231 cells which were engineered to upregulate SLC5A8 expression by treatment with DNMT inhibitors and then exposed to butyrate or pyruvate. (E) [C^{14}]-nicotinate uptake, which measure SLC5A8 function, of sodium dependent (NaCl) and independent (NMDGCl) in human metastatic breast cancer cell line M4 in the presence and absence of siRNA against HRAS and C/EBPβ, MEK-inhibitor (U0126), DNMTs inhibitors (5-AzaDC and P-NH2). (F) Similarly, sodium dependent (NaCl) and independent (NMDGCl) [C^{14}]-nicotinate uptake in human metastatic breast cancer cell line MB231 in the presence and absence of siRNA against HRAS and C/EBPβ, MEK-inhibitor (U0126), DNMTs inhibitors (5-AzaDC and P-NH2). Data are means ± SEM of three independent experiments. *$p<0.05$; **$p<0.01$ ***$p<0.001$ by t-test.

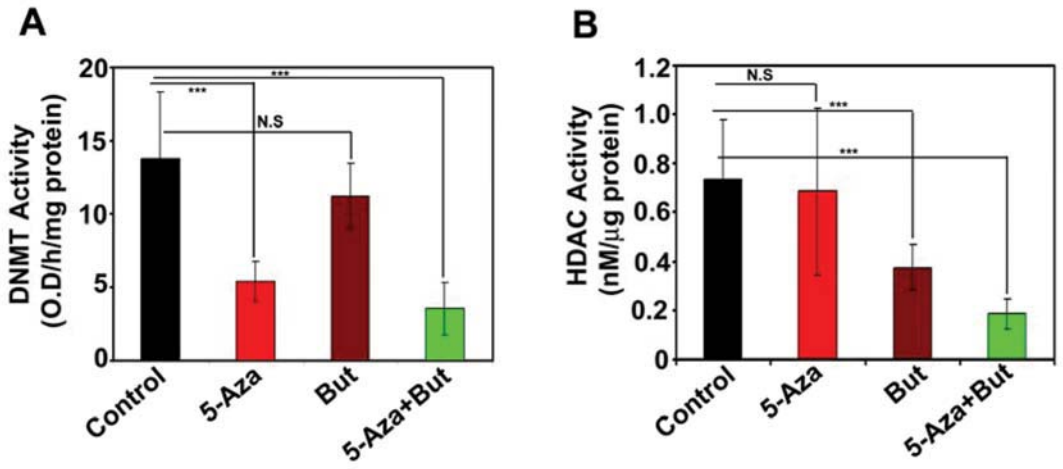

Figure S15

FIG S15 Administration of 5'-azacytidine and butyrate to mice via implantation of slow-releasing pellets decreased DNMT activity (A) and HDAC activity (B) in mammary gland, respectively. Data are means ± SEM (number of mice in each group = 12). **p<0.01; ***p<0.001 by t-test.

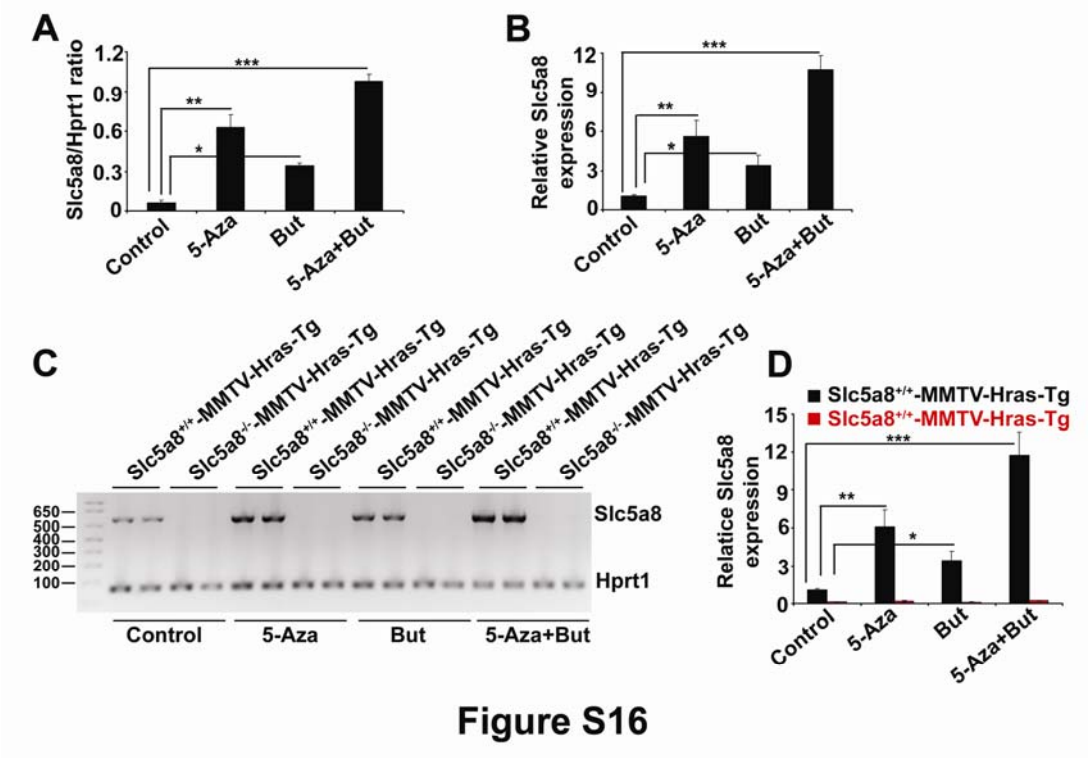

Figure S16

FIG S16 Administration of 5'-azacytidine and butyrate to mice via implantation of slow-releasing pellets reactivates Slc5a8 expression. (A) Qnantification of Slc5a8 and Hprt1 ratio in control, 5-Aza, But and combination of 5-Aza plus But treatment in Slc5a8$^{+/+}$-MMTV-Hras-Tg mice were assessed by semi-quantitative PCR analysis as shown Figure 7D insert. Data are means ± SEM (number of mice in each group = 12). *p<0.05; **p<0.01 ***p<0.001 by t-test. (B) qPCR data for Slc5a8 expression in control, 5-Aza, But and combination of 5-Aza plus But treatment in Slc5a8$^{+/+}$-MMTV-Hras-Tg were assessed by real-time PCR analysis. Data are means ± SEM (number of mice in each group = 12). *p<0.05; **p<0.01 ***p<0.001 by t-test. (C) Slc5a8 expression in control, 5-Aza, But and combination of 5-Aza plus But treatment in Slc5a8$^{+/+}$-MMTV-Hras-Tg and Slc5a8$^{-/-}$-MMTV-Hras-Tg mice were assessed by semi-quantitative PCR analysis. (D) qPCR data Slc5a8 expression in control, 5-Aza, But and combination of 5-Aza plus But treatment in Slc5a8$^{+/+}$-MMTV-Hras-Tg and Slc5a8$^{-/-}$-MMTV-

Hras-Tg mice were assessed by real-time PCR analysis. Data are means ± SEM (number of mice in each group = 12). **p<0.01; ***p<0.001 by t-test.

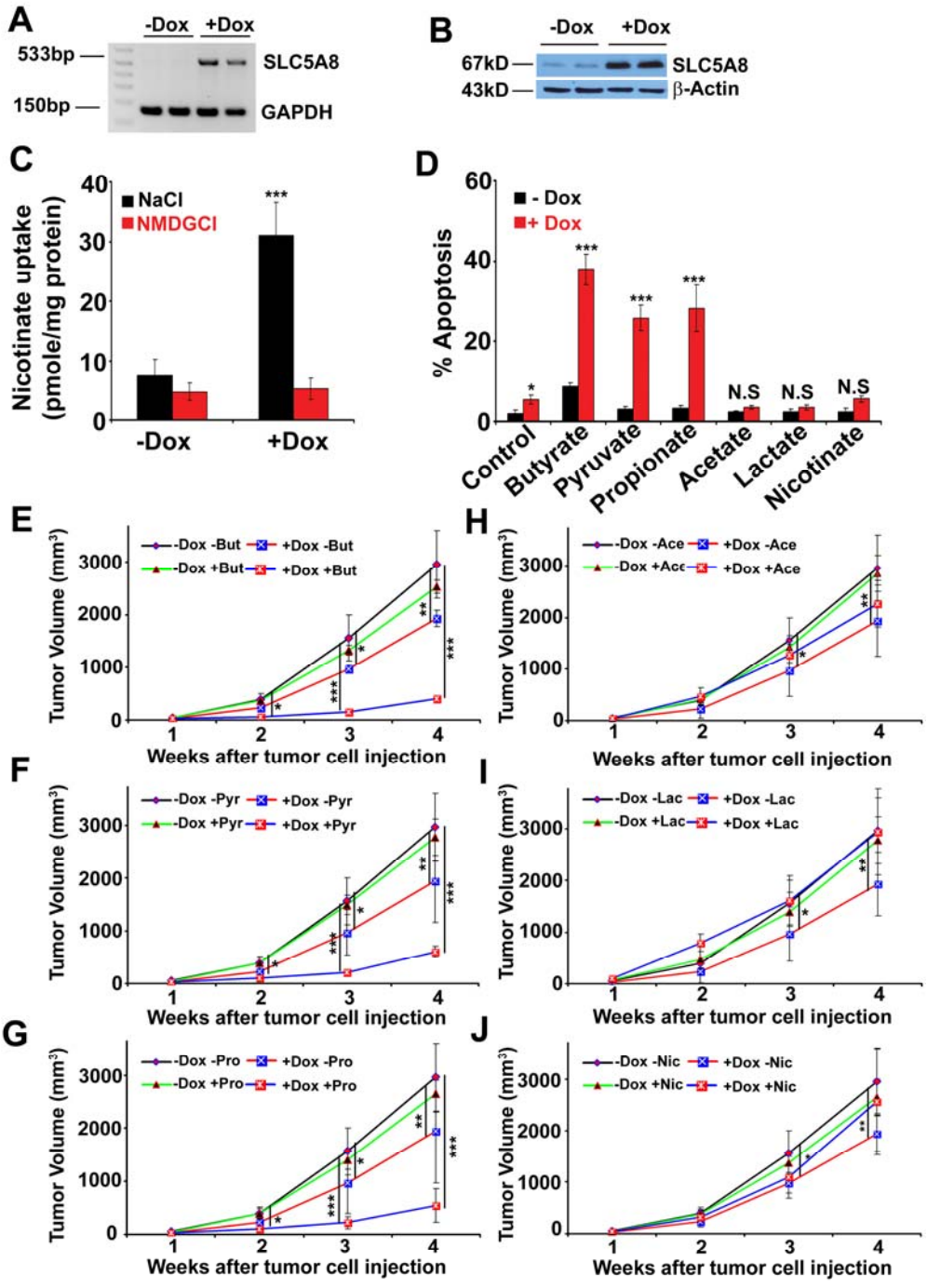

Figure S17

FIG S17 SLC5A8-induced tumor suppression is mainly associated with its transportable substrates, which inhibits HDACs. SLC5A8-pLVX stable clones were transfected in human metastatic breast cancer cell line M4 and SLC5A8 gene transcript by semi-quantitative-PCR (A), SLC5A8 protein expression by western blot (B) and SLC5A8 function by [C^{14}]nicotinate uptake (C) were measured in the presence and absence of doxycycline. (D) M4-SLC5A8-pLVX stable cell line was treated with doxycycline (2μg/ml) for 24 h to induce SLC5A8 and then treated with butyrate, pyruvate, and propionate (which inhibits HDACs) as well as with acetate, lactate and nicotinate (which do not inhibits HDACs) for 48 h. Propiodium iodide (PI) labeled cells were assessed in FACS analysis and quantified the subG0/1 cells, which are apoptotic cell population. Data are means ± SEM of three independent experiments. *$p<0.05$; ***$p<0.001$; N.S=Not significant by t-test. (E-J) Mouse xenograft was generated using the M4-SLC5A8-pLVX stable cell line ($1x10^7$ cells in 100 μl PBS, six mice in group). SLC5A8 expression was induced by doxycycline (2mg/ml) in drinking water on the same day of tumor cell implantation. After 48 h of tumor cell implantation, mice were treated with or without butyrate, pyruvate, propionate, acetate, lactate and nicotinate (2mg/ml in drinking water) for 4 weeks. Mice that do not treated with either doxycycline or SLC5A8 substrates kept as a control in all groups. Tumor volume was measured every week and tumor volume was calculated using the formula (width2×length)/2. Data are means ± SEM (number of mice in each group = 6). *$p<0.05$; **$p<0.01$; ***$p<0.001$ by t-test.

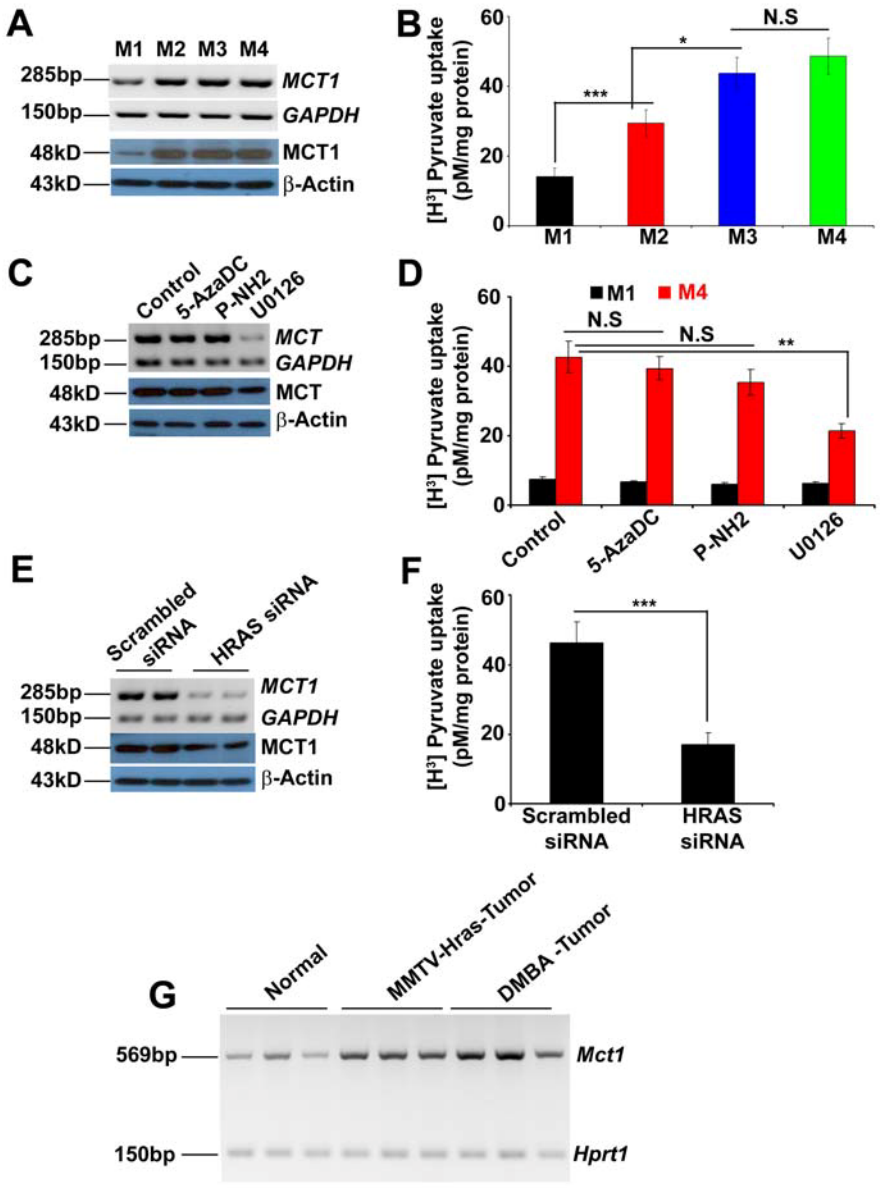

Figure S18

FIG S18 Oncogenic HRAS activates MCT1 expression and function. (A) Semi-quantitative and western blot analysis showing that oncogenic HRAS expression, in human non-transformed normal mammary epithelial cell line (M1) and associated series of isogenic transformed (M2), primary hyperplastic ductal (M3) and metastatic (M4) breast cancer, induced *MCT1* gene transcript and protein expression. (B) [H^3] pyruvate uptake showing that oncogenic HRAS

expression induced MCT function. (C) Treatment of M4 cells with DNMT inhibitors, 5-AzaDC and P-NH2 did not affect *MCT1* gene transcript and protein expression while MEK-inhibitor, U0126, inhibits *MCT1* gene transcript and protein expression. (D) Similarly, DNMT inhibitors did not affect MCT function while MEK-inhibitor reduced MCT uptake. However, both DNMT and MEK inhibitors did not affect MCT function in non-transformed normal cell line (M1). (E-F) HRASsiRNA inhibits *MCT1* gene transcript, MCT1 protein expression and MCT function. From A-F, Data are means ± SEM three independent experiments. *$p<0.05$; **$p<0.01$; ***$p<0.001$ by t-test. (G) Semi-quantitative PCR analysis showing the increased *Mct1* expression tumor tissues obtained from *MMTV-Hras-Tg* mouse and DMBA-induced mammary tumor than the normal mammary tissues. Data are shown representative images of 3 mice in each group.